Short and Medium-Range Order in Liquid Ternary $Al_{80}Co_{10}Ni_{10}$, $Al_{72.5}Co_{14.5}Ni_{13}$, and $Al_{65}Co_{17.5}Ni_{17.5}$ Alloys

Oleksandr S. Roik, Oleksiy Samsonnikov, Volodymyr Kazimirov, and Volodymyr Sokolskii

Chemical Department, National Taras Shevchenko University of Kyiv, 64 Volodymyrska Str., Kyiv, UA-01033, Ukraine

Reprint requests to O. S. R.; Fax: +38-0-44-23-93-417; E-mail: sasha78@univ.kiev.ua

A local short-to-intermediate range order of liquid $Al_{80}Co_{10}Ni_{10}$, $Al_{72.5}Co_{14.5}Ni_{13}$, and $Al_{65}Co_{17.5}Ni_{17.5}$ alloys was examined by X-ray diffraction and the reverse Monte Carlo modelling. The comprehensive analysis of three-dimensional models of the liquid ternary alloys was performed by means of the Voronoi-Delaunay method. The existence of a prepeak on the $S(Q)$ function of the liquid alloys is caused by medium range ordering of $3d$-transition metal atoms in dense-packed poly-tetrahedral clusters at temperatures close to the liquidus. The non-crystalline clusters, represented by aggregates of pentagons that consist of good tetrahedra, and chemical short-range order lead to the formation of the medium range order in the liquid binary Al-Ni, Al-Co and ternary Al-Ni-Co alloys.

Key words: High-Temperature Alloys; Atomic Scale Structure; X-Ray Diffraction;
Computer Simulations; Prepeak.

1. Introduction

Quasicrystalline (QC) phases possess attractive properties making them prominent for the adaptation in modern industries operating with metal alloys [1]. The QC phases can be obtained from the liquid binary Al-TM (TM – IIId transition metal) and liquid ternary Al-TM_1-TM_2 alloys by rapid quenching [2]. Therefore, the study of the connection between a short and a medium-range order in melts and corresponding quasicrystals and their approximants is particularly relevant for quasicrystal-forming in Al-based systems. With the increasing number of research works, devoted to study the atomic structure of liquid Al-based alloys, some features begin to attract more and more attention. The first feature is a prepeak in the $S(Q)$ function at the low-Q side of the first peak. The second one is a dominance of the icosahedral short-range order (ISRO) in undercooled Al-TM and Al-TM_1-TM_2 melts.

The presence of a prepeak in the structure factors of the liquid Al-based alloys with transition metals was reported in [3 – 11]. Prepeaks observed in the structure factors of liquid alloys at small Q-values are generally attributed to the medium-range order (MRO) in liquid alloys [8 – 10]. The prepeak in the structure factor (SF) curves of liquid Al-Ni and Al-Fe alloys was explained in [4, 5], caused by atomic clusters, the composition of which corresponds to the stoichiometry of the solid intermetallide Al_3Ni_2 and Al_5Fe_2, correspondingly. Maret et al. [7] explained prepeak phenomena of liquid $Al_{80}Ni_{20}$ alloy to be attributed to the Ni-Ni pairs related to a superstructure caused by Al-Ni interactions. The molecular dynamics (MD) simulations of the liquid binary Al-Ni alloys [10] showed a prepeak, manifesting itself in the partial structure factors $S_{NiNi}(Q)$ of the Al-rich compositions and in the $S_{AlAl}(Q)$ of Ni-rich compositions. A undercooled $Al_{13}(Co, Fe)_4$ melt was studied by D. Holland-Moritz et al. [8] by neutron diffraction using the isomorphous substitution of Co by Fe. The Faber-Ziman structure factors $S_{AlAl}(Q)$, $S_{AlTM}(Q)$, and $S_{TMTM}(Q)$ were obtained from three neutron scattering experiments with different scattering contrast of the components. The prepeak appeared on the $S_{TMTM}(Q)$ curve at low Q-values. Prepeak's existence on the partial structure factor $S_{TMTM}(Q)$, obtained at neutron scattering studies of the liquid $Al_{13}(Co_xFe_{1-x})_4$ (with $x = 1, 0.75, 0.5, 0.25, 0$) alloys [9], was testified. D. Holland-Moritz et al. [8] and T. Schenk et al. [9] considered the prepeaks to be a sign of chemical order. The formation of Al-TM pairs is preferable in the first coordination shell, while formation of TM-TM ones is avoided.

Neutron scattering studies and molecular dynamics simulations were performed above the liquidus temperature in the liquid $Al_{60}Mn_{40}$ and liquid quasicrystal-forming $Al_{80}Mn_{20}$ and $Al_{71}Pd_{19}Mn_{10}$ alloys [12]. Molecular dynamics studies showed the dominance of ISRO in these liquids. The short-range order (SRO) of undercooled and stable melts of Ni, Co, Zr, Fe, and $Al_{65}Cu_{25}Co_{10}$ was studied by neutron scattering and energy dispersive X-ray diffraction [13]. According to the SRO study in these melts, $S(Q)$ was simulated, assuming that the melt contains tightly bound clusters of the following structures: icosahedral, dodecahedral, fcc, hcp, and bcc. All these studies prove that an ISRO prevails in undercooled melts. The ISRO gets more pronounced on temperature decreasing. Information about icosahedral local order was also obtained by such a simulation method for other melts. Similar studies of the ISRO have been carried out for liquid Ti-Zr-Ni [14], Al-Pd-Mn [15, 16], $Al_{92.3}Mn_{7.7}$, $Al_{81}Pd_{19}$, $Al_{72.1}Pd_{20.7}Mn_{7.2}$, and $Al_{88.5}(Mn_xCr_{1-x})_{11.5}$ ($0 < x < 1$) alloys [17]. The icosahedral short-range order was accompanied by a chemical short-range order so, that the first coordination shell of a transition metal atom consists preferentially of Al atoms [8, 9, 17, 18].

The X-ray diffraction studies and simulations of the local atomic structure, being a function of the alloy composition, in the liquid binary Al-Co and Al-Ni alloys have been performed earlier [19]. The present paper is devoted to examine the selected ternary alloys with compositions of $Al_{80}Co_{10}Ni_{10}$, $Al_{72.5}Co_{14.5}Ni_{13}$, and $Al_{65}Co_{17.5}Ni_{17.5}$. Two of the alloys ($Al_{80}Co_{10}Ni_{10}$ and $Al_{65}Co_{17.5}Ni_{17.5}$) beyond the field of QC phase formation and the $Al_{72.5}Co_{14.5}Ni_{13}$ alloy belonging to the field of QC phase formation [20] were studied at 1473 K and at 1473 K, 1533 K, and 1673 K, respectively. The study of the atomic structure of the liquid ternary Al-Ni-Co alloys includes the following steps: the diffraction experiment with a maximal possible accuracy, the correct calculations of structure factor (SF) and total pair correlation function (TPCF), the reconstruction of the 3D-models of the liquid alloys from the SF experimental curves using the reverse Monte Carlo (RMC) method [21], and the analysis of the local and medium-range atomic ordering by means of the Voronoi diagram and the Delaunay tessellation [22]. The local and the medium-range atomic ordering in the ternary Al-Ni-Co liquid alloys should be comparatively analyzed taking in account the ordering in the binary Al-Co(Ni) liquid alloys.

2. Experimental

2.1. Ternary Alloys Preparation

The ternary $Al_{80}Co_{10}Ni_{10}$, $Al_{72.5}Co_{14.5}Ni_{13}$, $Al_{65}Co_{17.5}Ni_{17.5}$ alloys were prepared from high purity materials: aluminium (99.999 wt. %), cobalt (99.8 wt. %), and nickel (99.8 wt. %). Weighed amounts of the pure elements taking in ratios appropriate to the nominal compositions were arc-melted under a protective argon atmosphere. The arc-melting process was repeated several times to ensure a complete homogenization of the alloys. The ternary alloys obtained were removed from the furnace and quenched.

2.2. Diffraction Study of the Liquid Ternary Alloys

The ternary alloys prepared were transfered into the alumina crucibles and placed into a stainless steel chamber. The chamber inner volume was vacuumized and filled with pure helium. A special resistant heater inserted into the chamber was used for the progressive heating of the alloys up to the experimental temperature in helium atmosphere. X-Ray diffraction measurements were performed at different temperatures (all above liquidus with an accuracy of ±5 K using a θ-θ diffractometer (MoK_α-radiation, $\lambda = 0.071069$ nm). The apparatus and the measurement routines were previously reported in [23]. The magnitude of the experimental diffraction vector ($Q = 4\pi \sin\theta/\lambda$, where θ is the half of the scattering angle) was ranged from 9 to 125 nm^{-1}. Three sets of diffraction data were collected for each of the liquid ternary alloys in order to minimize random errors. The scattering intensity measured in arbitrary units were converted into the coherent scattering intensity per atom in electron units $I^{coh}(Q)$ using the methodology proposed in [24], and were corrected for the polarization and the angular dependence of Compton scattering [25]. The total structure factor $S(Q)$ was obtained as

$$S(Q) = I^{coh}(Q)/(N\Sigma c_i f_i^2), \tag{1}$$

where $I^{coh}(Q)$ is the scattered intensity at the diffraction vector Q for N atoms, c_i and f_i are the concentration and the atomic scattering factor of the component atoms i, respectively. The total pair correlation function $g(r)$ was obtained as Fourier transform of $S(Q)$:

$$g(r) = 1 + \frac{1}{2\pi^2 r \rho_0 (\sum_i c_i K_i)^2}$$
$$\cdot \int_{Q_{\min}}^{Q_{\max}} Q[S(Q) - 1] \sin(Qr) dQ, \quad (2)$$

where ρ_0 is the average density, $K_i^2 = f_i^2 / F^2$ ($F^2 = \sum_i c_i f_i^2$).

2.3. Reverse Monte Carlo (RMC) Simulation

The liquid alloy simulation was performed using RMC modelling [21]. A basic cubic cell was arranged with 10^4 spherical symmetric particles with the imposed periodical boundary conditions. The density ρ of the liquid ternary alloys at the temperature of X-ray diffraction study were estimated by

$$\rho(Al_{1-x-y}Co_x Ni_y) = (Al_{1-x-y}Co_{x+y}) \frac{x}{x+y}$$
$$+ (Al_{1-x-y}Ni_{x+y}) \frac{y}{x+y}. \quad (3)$$

Experimental ρ values for the binary alloys were taken from [26]. The cut-off distances $d_{Al-Al} = 0.23$ nm, $d_{Ni-Ni} = 0.21$ nm, and $d_{Co-Co} = 0.21$ nm, obtained from the experimental $g(r)$ functions of pure liquid metals, were used as constrains in the RMC simulations. The cut-off distances between different atoms were calculated as arithmetic mean of the pure metals cut-offs. According to the RMC algorithm, the iterative process proceeds until the discrepancy χ^2 between experimental $S^{\exp}(Q)$ and simulated $S^{\sim}(Q)$ structure factors becomes a smaller equilibrium value

$$\chi^2 = \sum_{i=1}^{N} \left(S^{\sim}(Q_i) - S^{\exp}(Q_i) \right)^2 / \sigma^2(Q_i), \quad (4)$$

where i is the number of points in the diagram of the structure functions and $\sigma^2(Q_i)$ is the experimental error as a function of diffraction vector Q. The statistical error of the $S^{\exp}(Q)$ function counting was found to be 1%. Three-dimensional models of the liquid alloys reproducing the experimental structure factors were obtained as RMC modelling result. From these models, the partial pair correlation functions $g_{ij}(r)$ and the corresponding partial structure factors $S_{ij}(Q)$ were obtained.

The analysis of the RMC simulated models was performed by means of the Voronoi-Delaunay method [10], dividing the model space into Voronoi polyhedra

(VP) and Delaunay simplexes (DS). The Voronoi diagram and the Delaunay tessellation were realized using the algorithm proposed in [27]. The model space was dissected into polyhedrons, and the coordinates of the polyhedron vertices are determined as

$$(x_i - x)^2 + (y_i - y)^2 + (z_i - z)^2 = R^2 + R_i^2, \; i = 1-4, \; (5)$$

where x, y, z are the coordinates of a polyhedron vertex; x_i, y_i, z_i, R_i are the coordinates and the atomic radii ($R_{Al} = 0.115$, $R_{Co} = 0.105$, $R_{Ni} = 0.105$ nm) of the four atoms nearest to the vertex (the Delaunay simplex); and R is the radius of the circumscribed sphere around those atoms.

The sensitivity of the VP statistical analysis to the features of a short-range order enables to examine statistical regularities of the local atomic arrangement in liquid metals and alloys [28]. The medium-range order in simulated configurations was studied by percolating the network composed of the DS's. The tetrahedrisity parameter T [29] used to select dense packing clusters was calculated as

$$T = \sum_{i \neq j} (l_i - l_j)^2 / 15 l_0^2, \quad (6)$$

where l_i and l_j are the lengths of the simplex edges, and l_0 is the mean edge length. If the T value tends to zero, the simplex tends to a regular tetrahedron. To analyze atom arrangements, the Delaunay simplexes with $T \leq 0.018$, corresponding to the minimum in the T-distribution for heated fcc-crystal, were selected. Bonded centers of the DS's, which were selected by T, form the densed packed cluster, whose structure will be examined in details below.

3. Results and Discussion

3.1. Results of X-Ray Diffraction Studies

SFs and TPCFs of the ternary liquid alloys are represented in Figure 1. As one can see from Figures 1a and c, a prepeak at $13 < Q/nm^{-1} < 21$ and four peaks at $Q > 22$ nm^{-1} are observed on the SFs curves. The prepeak appears at lower temperature and disappears with temperature increase (Fig. 1c). All SF curves of liquid Al$_{80}$Co$_{10}$Ni$_{10}$ and Al$_{72.5}$Co$_{14.5}$Ni$_{13}$ alloys are characterized by the irregular shape of the third peak. This third peak in the case of Al$_{72.5}$Co$_{14.5}$Ni$_{13}$ alloys splits at 1473 K, thus this splitting smooths at heating with changings in the liquid structure (Fig. 1c).

Table 1. Structural parameters for the liquid alloys.

Composition	T [K]	Q_1 [nm^{-1}]	$S(Q_1)$	R_1 [nm]	Q_{pp} [nm^{-1}]	W [%]	R_{pp} [nm]
Al [19]	973	26.7	1.97	0.278			
Al$_{82}$Ni$_{18}$ [19]	1403	29.7	1.93	0.257	18.7	19	0.41
Al$_{80}$Co$_{20}$ [19]	1403	29.7	2.27	0.256	17.5	16	0.44
Al$_{80}$Co$_{10}$Ni$_{10}$	1473	29.5	2.25	0.253	18.8	17	0.41
Al$_{72}$Ni$_{28}$ [19]	1423	29.9	2.06	0.253	19.0	21	0.41
Al$_{71.43}$Co$_{28.57}$ [19]	1593	30.4	2.19	0.252	18.5	7	0.42
	1473	30.1	2.14	0.249	18.7	17	0.41
Al$_{72.5}$Co$_{14.5}$Ni$_{13}$	1533	29.6	2.13	0.250	17.8	9	0.43
	1673	29.0	2.12	0.251	15.2	10	0.50
Al$_{68}$Ni$_{32}$ [19]	1653	29.8	1.92	0.250	19.1	24	0.40
Al$_{65}$Co$_{17.5}$Ni$_{17.5}$	1473	30.2	2.14	0.247	19.2	19	0.40
Al$_{60}$Ni$_{40}$ [19]	1773	30.5	1.85	0.247	19.5	25	0.40
Co [19]	1803	30.5	2.83	0.246			
Ni [19]	1823	30.6	2.75	0.243			

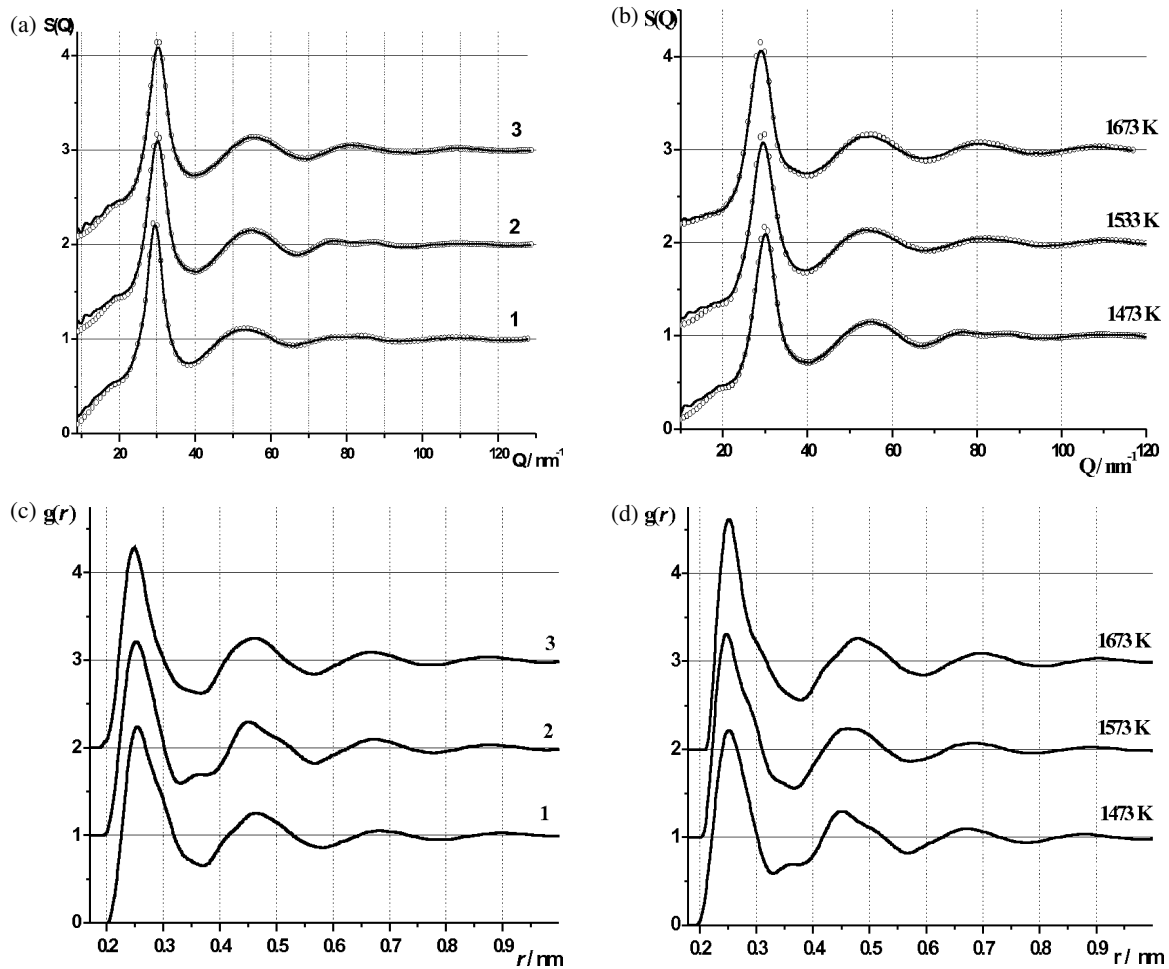

Fig. 1. Structure factor (SF) (a, b) and total pair correlation function (TPCF) (c, d) of the liquid ternary alloys. (a, c): 1 – Al$_{80}$Co$_{10}$Ni$_{10}$, 2 – Al$_{72.5}$Co$_{14.5}$Ni$_{13}$, 3 – Al$_{65}$Co$_{17.5}$Ni$_{17.5}$ at 1473 K and (b, d): Al$_{72.5}$Co$_{14.5}$Ni$_{13}$ at different temperatures. For the SFs (a, b) open circles are experimental data, solid lines are data calculated for the reverse Monte Carlo configuration (RMC). For the TPCF (c, d) solid lines are the experimental data.

All the TPCFs of the ternary alloys show a second peak asymmetry, the last testifies on the existence of a more compact structure formed by a certain part of atoms in the liquid alloys. The nature of this effect is discussed hereinafter. The structural parameters for the liquid alloys including the main peak positions (Q_1), their heights $S(Q_1)$, and the main peak positions (R_1) determined from the SF and TPCF curves, respectively, are listed in Table 1.

The structural parameters for the binary and uninary liquid alloys studied earlier [19] are represented in Table 1 for comparison. If the structure parameters (Q_1 and R_1) of liquid binary Al-Ni(Co) and ternary Al-Co-Ni alloys are compared with the ones of liquid Al ones, the addition of Ni(Co) effects on the short-range order of liquid Al. The dependence of R_1 from the Al content in the binary and ternary alloys is characterized by negative deviations from a linear (Table 1) highlighting preference in strong interactions between Al and Ni(Co) atoms. The distances R_1 for the liquid Al-Co-Ni alloys are less than that for the liquid Al-Ni(Co) alloys, considering the alloys with the same Al content, that indicates a strengthening of the interatomic interactions.

If focused on the SFs, the special attention should be paid to the prepeak analysis. The prepeaks observed in the structure factors for small Q-values are generally attributed to medium-range order (MRO) in liquid alloys. The MRO is defined by the order extending up to larger nearest interatomic distances in the noncrystalline state in contrast to those corresponding to the local short-range order. It was shown [19] that the prepeak in the structure factor curve of the liquid binary Al-Ni and Al-Co alloys is caused by a specific arrangement of transition metal atoms in dense-packed polytetrahedral clusters.

Analyzing experimental SFs, the prepeaks positions (Q_{pp}) and heights $S(Q)$ were determined by subtracting the main maximum background. The main maximum and the prepeak in the SF curves were fitted by means of pseudo-Voigt functions:

$$F(\Delta Q) = \begin{cases} h \cdot e^{-b(\Delta Q)^2} & \text{for } (\Delta Q)^2 < \dfrac{\ln 2}{b} \\ \dfrac{0.5h}{1 - \ln 2 + b(\Delta Q)^2} & \text{for } (\Delta Q)^2 < \dfrac{\ln 2}{b} \end{cases}, \quad (7)$$

where $\Delta Q = Q - Q_M$, Q_M is the position of a peak, h is the peak height, and $b = 2.772/l$ (where l is the half-width of the peak). To estimate the interatomic

distances R_{pp} in the TPCFs which correspond to the position of the prepeak (Q_{pp}) in $S(Q)$, the empirical equation proposed by Ehrenfest [30] has been used:

$$Q_{pp} \cdot R_{pp} = 1.23 \cdot 2\pi. \quad (8)$$

The R_{pp} values (Table 1) are in a good agreement with the position of shoulder maximum in the second peak on the experimental TPCF (Fig. 1b, d). The ratio $W = A_{pp}/A_{main}$, where A_{pp} and A_{main} are the areas of the prepeak and the main peak in the $S(Q)$ curve, respectively, reflects the proportion of the structures corresponding to the prepeak and to the local short-range order. The position of prepeak and W calculated for the liquid ternary alloys remains to be constant with the increase of Ni or/and Co content, but Q_{pp} and W change with temperature increase (Table 1).

3.2. Analysis of RMC Simulation Results

The simulated and the experimental $S(Q)$ functions coincide satisfactory (Fig. 1a, c). The partial structure factors $S_{ij}(Q)$ obtained from the RMC models show that the prepeak has been observed on the $S_{NiNi}(Q)$, $S_{CoCo}(Q)$, and $S_{NiCo}(Q)$ curves. Co and Ni have a very close X-ray scattering cross section. Therefore a determination of partial Co-Co, Ni-Ni or Co-Ni structure factors by the RMC method using the experimental data is incorrect. Because of the fact, that the shape and position of the maximums of $S_{NiNi}(Q)$, $S_{CoCo}(Q)$, and $S_{NiCo}(Q)$ curves are close, we have replaced them by $S_{TMTM}(Q)$ using a quasi-binary approach:

$$\begin{aligned} S_{TMTM}(Q) - 1 = & \frac{c_{Ni}^2 f_{Ni}^2(Q)(S_{NiNi}(Q) - 1)}{(c_{Ni}f_{Ni}(Q) + c_{Co}f_{Co}(Q))^2} \\ & + \frac{n_{Ni}n_{Co}f_{Ni}(Q)f_{Co}(Q)(S_{NiCo}(Q) - 1)}{(c_{Ni}f_{Ni}(Q) + c_{Co}f_{Co}(Q))^2} \\ & + \frac{n_{Co}^2 f_{Co}(Q)(S_{CoCo}(Q) - 1)}{(c_{Ni}f_{Ni}(Q) + c_{Co}f_{Co}(Q))^2}, \quad (9) \end{aligned}$$

where c_i and $f_i(Q)$ are the concentration and the atomic scattering factor of the i-th component atoms. Using the RMC method, the ordering of TM atoms has been considered without indicating whether the atom is Co or Ni, that solves the problem of partial structure factors determination correctness. The partial pair distribution functions $g_{TMTM}(r)$ were obtained by using the Fourier transformation of $S_{TMTM}(Q)$.

The partial structure factors $S_{TMTM}(Q)$ and pair correlation functions $g_{TMTM}(r)$ are shown in Figure 2. The

Table 2. Values of the average $[K_{sph}]$ and the standard deviation (σ) for K_{sph} distribution of VP.

Composition	T [K]	— $[K_{sph}]$ —			— σ [%] —		
		Al	Ni	Co	Al	Ni	Co
$Al_{80}Co_{10}Ni_{10}$	1473	0.674 ± 0.001	0.679	0.676	4.56 ± 0.05	4.64	4.29
	1473	0.676	0.668	0.670	4.37	4.66	4.76
$Al_{72.5}Co_{14.5}Ni_{13}$	1533	0.685	0.685	0.683	3.86	4.26	4.09
	1673	0.688	0.684	0.686	3.63	4.04	4.05
$Al_{65}Co_{17.5}Ni_{17.5}$	1473	0.689	0.672	0.674	3.50	4.18	4.09
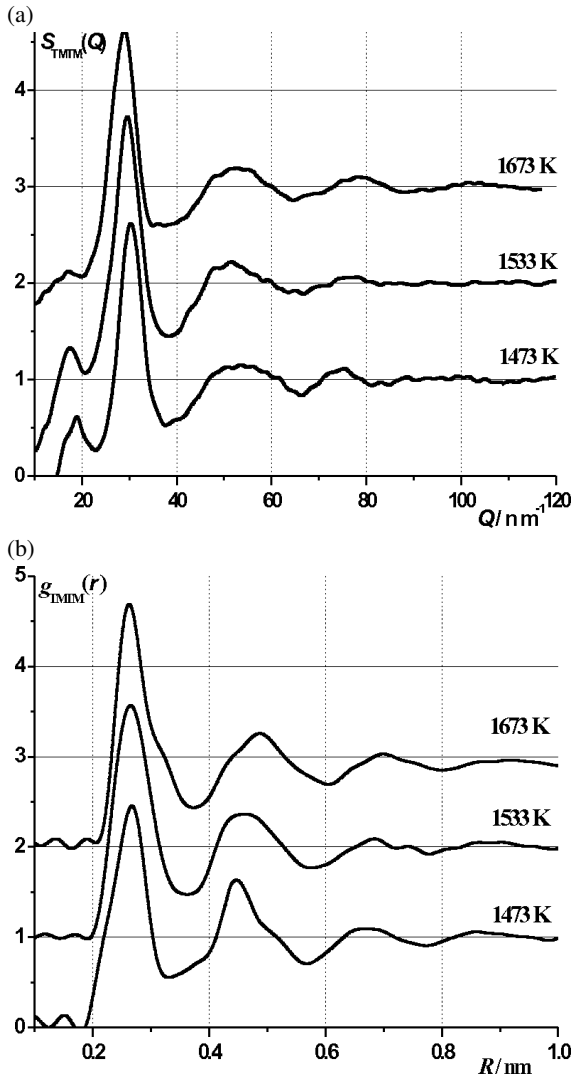
Fig. 2. Partial structure factors $S_{TMTM}(Q)$ (a) and pair correlation functions $g_{TMTM}(r)$ (b) of the liquid ternary $Al_{72.5}Co_{14.5}Ni_{13}$ alloy at different temperatures.

prepeak in the experimental structure factor curve can also be interpreted as a correlation in the arrangement of TM atoms in melts. This fact goes with molecu-

lar dynamics simulations [7, 10] and neutron diffraction studies [8, 9] of Al-TM and Al-TM$_1$-TM$_2$ melts. In our opinion, the results of the RMC simulations of the Al-Ni-Co melts, obtained by using the measured total structure factors, are unique enough.

The R_{pp}(TM–TM) values were calculated from (8) and found to be in a range of 0.42 – 0.44 nm. The partial pair correlation functions $g_{TMTM}(r)$ are characterized by a pronounced height of the second peak, which is localized in the range of 0.43 – 0.45 nm. The amplitude of the first peak of $g_{TMTM}(r)$ decreases with decreasing temperature (Fig. 2). In contrast, the amplitude of the second peak increases with decreasing temperature and becomes close to the first one. This fact goes with the results of Schenk et al. [9]. So, one can conclude that the TM atoms in the RMC simulated model have been located in the second coordination sphere of the TM atoms, suggesting a repulsion of TM-TM first neighbours. The primary localization of Al-atoms in the first coordination sphere of TM atoms indicates the chemical short-range order in the Al-Ni-Co melts. On the other hand, the prepeak in the SFs indicates ordering beyond the first few nearest neighbour distances between TM atoms, corresponding to MRO. The MRO and prepeak on the experimental $S(Q)$ are accompanied by a chemical short-range order (CSRO) in the melts. This CSRO is enhanced with temperature decreasing, that is not surprising.

The short-range order of the models was analyzed using the metric and the topological characteristics of Voronoi polyhedra (VP). It was found that the most informative metric characteristic of VP is the sphericity coefficient K_{sph}. The K_{sph} distributions of all studied models were obtained. The most probable values of the sphericity coefficient $[K_{sph}]$ and the standard deviation σ of the K_{sph} distribution characterizing the prevailing types of the local ordering, were calculated by $K_{sph} = 36\pi V^2/S^3$, where V is the volume and S the surface area of the Voronoi polyhedron, and listed in Table 2. These values were calculated for VP containing Al or Co(Ni) atoms as a center. The low value of $[K_{sph}]$
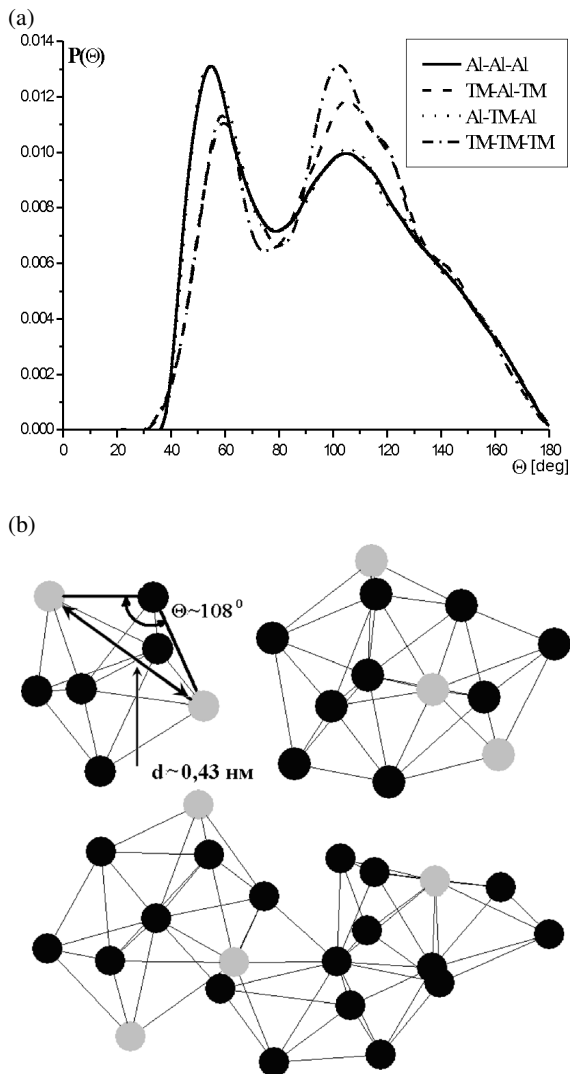
(a)

(b)

Fig. 3. Probability of the bond angle distribution in liquid $Al_{80}Co_{10}Ni_{10}$ melt at 1473 K (a) and the typical polytetrahedral clusters, which exist in the liquid ternary alloys (b). The black circles: Al; gray circles: Ni(Co) atoms.

together with the high value of σ may be attributed to a low packing density of atoms in the liquid. The $[K_{sph}]$ and σ calculated for the liquid $Al_{72.5}Co_{14.5}Ni_{13}$ alloy shift considerably when temperature increases from 1473 to 1533 K. That quantitatively confirms the temperature dependence of the CRSO discussed before. This fact is in a good agreement with the disappearing of the prepeak with increasing temperature (Fig. 1c and Table 1).

The dense packing of atoms in liquid ternary alloys and the CSRO are interrelated and opposite cases of

liquid alloy ordering. At heating the dense packing of atoms in the liquid ternary alloys increases decreasing the CSRO, that is observed experimentally as the prepeak intensity decrease in the SFs.

The percolation analysis of the network consisting of the Delaunay simplexes has shown specific ordering of TM atoms in polytetrahedral clusters. These clusters are presented by aggregates of pentagons consisting of close to perfect tetrahedra, which are adjacent by faces. Atomic centers in pentagon form vertices of a pentagonal bipyramid (ten-faced body), known as decahedron in geometry [22]. Aggregation of several decahedrons leads to formations of icosahedral-type clusters, which determines icosahedral short-range order (ISRO). Therefore the ISRO is a particular case of the general atomic ordering in dense-packed polytetrahedral clusters. Some polytetrahedral clusters obtained from RMC-model clusters of melts are shown in Figure 3.

Using the atomic configuration obtained by the RMC procedure, the statistics of the bond angles have been analyzed. All of the bond angle distributions show two peaks at around $55°$ and $108°$. For example, Figure 3a shows the bond angle distributions for Al-Al-Al, TM-Al-TM, TM-Al-TM, and TM-TM-TM obtained from RMC simulations for the $Al_{72.5}Co_{14.5}Ni_{13}$ melt. The bond angle distribution for the TM-Al-TM atoms shows a pronounced peak around $108°$ that is observed in the pentagons with alternating Al-Al and Al-TM bonds in the decahedron (Fig. 3b).

The distances $R(TM-TM)$ between TM atoms in the polytetrahedral clusters are found to be in the range of $0.41 - 0.45$ nm (Fig. 3b) and so making significant contribution into the PCF second peak. The distances range is in accord with the data obtained from (8) and with the partial $g_{TMTM}(r)$. It can be concluded that the CSRO and the formation of dense packing clusters is responsible for the MRO structure formation in the liquid ternary Al-Co-Ni alloys.

The CSRO of the liquid binary Al-Co, Al-Ni, and Al-Ni-Co alloys in the Al-rich region is reminiscent of one in the solid phases [31]. For example, the structure of Al-Co decagonal approximant phases has been described as being a dense-packed tenfold or fivefold symmetry decagonal cluster. These clusters are characterized by a decagonal ring of alternating aluminum and cobalt atoms, that correlates with our results. The pair distributions in monoclinic and orthorhombic $Al_{13}Co_4$ phases (decagonal phase approximants) exhibit a strong peak for the Al-Co pairs at

around 2.5 Å [31, 32]. Otherwise, Co-Co correlation corresponds to a larger distance of about 4.5 Å. The similar results have been obtained by Widom and Al-Lehyani [33] for the Co-Co and Al-Co correlations in the decagonal phase of Al-Co-Cu. Thus the presence of the dense-packed polytetrahedral clusters with specific chemical-short-order contributes to the appearance of QCs phases in the liquid Al-Co, Al-Ni, and Al-Ni-Co alloys.

The content of Al in the polytetrahedral clusters is lower than the content of Al in the total composition of the liquid ternary Al-Co-Ni alloys. This fact denotes a concurrence between TM and Al atoms for the position in a coordination environment of Al atoms, stabilizing these clusters. It is possible to assume, that the ability to QC-phase formation in the liquid Al-Co-Ni alloys concerned with the presence of icosahedral-type stable clusters, which composition differ from total composition of the liquid ternary alloys.

4. Conclusion

The X-ray diffraction studies and the RMC simulations of the liquid ternary $Al_{80}Co_{10}Ni_{10}$, $Al_{72.5}Co_{14.5}Ni_{13}$, and $Al_{65}Co_{17.5}Ni_{17.5}$ alloys have been performed. A strong interaction between Al and TM atoms in the liquid ternary alloys leads to a shortening of the nearest-neighbour distances (R_1) as compared with ones of the liquid binary Al-Ni(Co) alloys with the same Al content. The intensity of the prepeak at small Q-values decreases considerably with temperature increase. However, the prepeak intensity remains to be constant with the Al content decreasing in the liquid ternary alloys. In accordance with the results of the RMC simulation the prepeak can be caused by MRO in the dense packed polytetrahedral clusters which composition differ of the total composition of the liquid ternary alloys.

[1] J.-M. Dubois, Mater. Sci. Eng. A **294 – 296**, 4 (2000).

[2] W. Steurer, Z. Kristallogr. **219**, 391 (2004).

[3] M. Maret, A. Pasturel, C. Senillou, J. M. Dubois, and P. Chieux, J. Phys. (Paris) **50**, 295 (1989).

[4] E. A. Pastukhov, N. A. Vatolin, V. L. Lisin, V. M. Denisov, and S. V. Kachin, Ural Division, Russian Academy of Sciences, Ekaterinburg 2003.

[5] A. Il'inskii, S. Slyusarenko, O. Slukhovskii, I. Kaban, and W. Hover, Mater. Sci. Eng. A **325**, 98 (2002).

[6] J. Brillo, A. Bytchkov, I. Egry, L. Hennet, G. Mathiak, I. Pozdnyakova, D. L. Price, D. Thiaodiere, and D. Zanghi, J. Non-Cryst. Solids, **352**, 4008 (2006).

[7] M. Maret, T. Pomme, and A. Pasturel, Phys. Rev. B **42**, 1598 (1990).

[8] D. Holland-Moritz, T. Schenk, V. Simonet, and R. Bellissent, Philosophical Magazine **86**, 255 (2006).

[9] T. Schenk, V. Simonet, D. Holland-Moritz, R. Bellissent, T. Hansen, P. Convert, and D. M. Herlach, Europhys. Lett. **65**, 34 (2004).

[10] S. K. Das, J. Horbach, M. M. Koza, S. Mavila Chatoth, and A. Meyer, Appl. Phys. Lett. **86**, 011918 (2005).

[11] Q. Jingyu, B. Xiufang, S. I. Sliusarenkoy, and Wang Weiminy, J. Phys.: Condens. Matter **10**, 1211 (1998).

[12] M. Maret, F. Lancon, and L. Billard, J. Phys.: Condens. Matter **6**, 5791 (1994).

[13] D. Holland-Moritz, T. Schenk, V. Simonet, R. Bellissent, P. Convert, T. Hansen, and D. M. Herlach, Mater. Sci. Enging. A **375 – 377**, 98 (2004).

[14] K. F. Kelton, G. W. Lee, A. K. Gangopadhyay, R. W. Hyers, T. J. Rathz, J. R. Rogers, M. B. Robinson, and D. S. Robinson, Phys. Rev. Lett. **90**, 195504 (2003).

[15] V. Simonet, H. Hippert, H. Klein, M. Audier, R. Bellissent, H. Fischer, A. P. Murani, and D. Boursieret, Phys. Rev. B **58**, 6273 (1998).

[16] G. W. Lee, A. K. Gangopadhyay, R. W. Hyers, T. J. Rathz, J. R. Rogers, D. S. Robinson, A. I. and K. F. Kelton, Phys. Rev. B **77**, 184102 (2008).

[17] V. Simonet, F. Hippert, M. Audier, and R. Bellissent, Phys. Rev. B **65**, 024203 (2001).

[18] D. Holland-Moritz, G. Jacobs, and I. Egry, Mater. Sci. Eng. A **294 – 296**, 369 (2000).

[19] O. S. Roik, O. V. Samsonnikov, V. P. Kazimirov, and V. E. Sokolskii, J. Mol. Liq. **145**, 129 (2009).

[20] B. Grushko and M. Doblinger, Z. Kristallogr. **219**, 447 (2004).

[21] R. L. McGreevy, J. Phys.: Condens. Matter **13**, R877 (2001).

[22] N. N. Medvedev, Voronoi-Delaunay Method for Noncrystalline Structures, Siberian Division, Russian Academy of Science, Novosibirsk 2000.

[23] V. E. Sokol'skii, V. P. Kazimirov, and V. G. Kuzmenko, J. Mol. Liq. **93**, 235 (2001).

[24] W. Bol, J. Sci. Instr. **44**, 736 (1967).

[25] V. M. Avdyukhina, D. Batsur', V. V. Zubenko, A. A. Katsnel'son, S. S. Kvitka, and N. S. Kolesova, in: X-ray Diffraction Analysis. Special Practical Works (Ed. A. A. Katsnel'son), Gos. Univ., Moscow 1986, p. 24.

[26] G. D. Ayushina, E. S. Levin, and P. V. Gel'd, Zh. Fiz. Khim. **43**, 2756 (1969).

[27] N. N. Medvedev, J. Comput. Phys. **67**, 223 (1986).

[28] A. S. Roik, V. P. Kazimirov, and V. E. Sokolskii, J. Struct. Chem. **45**, 648 (2004).

[29] N. N. Medvedev and Y. I. Naberukhin, J. Non-Cryst. Solids **94**, 402 (1987).

[30] A. Guinier, Theorie et technique de la radiocristallographie, Dunot, Paris 1956.

[31] M. Widom and E. Cockayne, Physica A **232**, 713 (1996).

[32] M. Mihalkovic, H. Elhor, and J. B. Suck, Phys. Rev. B **63**, 214301 (2001).

[33] M. Widom and I. Al-Lehyani, Phys. Rev. B **62**, 3648 (2000).